Eur. Phys. J. E **19**, 195–202 (2006)
DOI: 10.1140/epje/e2006-00025-4

THE EUROPEAN PHYSICAL JOURNAL E

Viscosity effects in foam drainage: Newtonian and non-newtonian foaming fluids

M. Safouane[1], A. Saint-Jalmes[1,a], V. Bergeron[2], and D. Langevin[1]

[1] Laboratoire de Physique des Solides, Université Paris-Sud, 91405 Orsay, France
[2] Laboratoire de Physique, ENS Lyon, 69364 Lyon, France

Received 25 October 2005 / Received in final form 11 December 2005
Published online 28 February 2006 –

Abstract. We have studied the drainage of foams made from Newtonian and non-Newtonian solutions of different viscosities. Forced-drainage experiments first show that the behavior of Newtonian solutions and of shear-thinning ones (foaming solutions containing either Carbopol or Xanthan) are identical, provided one considers the actual viscosity corresponding to the shear rate found inside the foam. Second, for these fluids, a drainage regime transition occurs as the bulk viscosity is increased, illustrating a coupling between surface and bulk flow in the channels between bubbles. The properties of this transition appear different from the ones observed in previous works in which the interfacial viscoelasticity was varied. Finally, we show that foams made of solutions containing long flexible PolyEthylene Oxide (PEO) molecules counter-intuitively drain faster than foams made with Newtonian solutions of the same viscosity. Complementary experiments made with fluids having all the same viscosity but different responses to elongational stresses (PEO-based Boger fluids) suggest an important role of the elastic properties of the PEO solutions on the faster drainage.
PACS. 82.70.Rr Aerosols and foams – 47.60.+i Flows in ducts, channels, nozzles, and conduits – 47.56.+r Flows through porous media

1 Introduction

An aqueous foam drains under gravity: the liquid flows downward through the foam, and the foam liquid content irreversibly decreases with time [1]. At long times, most of the liquid is drained out of the foam, leaving it extremely dry and fragile. Drainage therefore plays a key role in the life time of the foam, and its understanding is thus crucial for foam applications.

Recently, two foam drainage regimes have been identified [2–8], which are related to different boundary conditions at the surface of the bubbles (*i.e.* mobile or immobile surfaces). Each regime corresponds to specific location of the viscous dissipation (or hydrodynamic resistance) in the foam structure. In the case of immobile rigid surfaces, the main resistance comes from the liquid channels (Plateau borders, PB) [2,3]; while in the case of mobile fluid surfaces, the main resistance arises from the nodes (junctions of Plateau borders) [4,5]. The difference in the geometry of these structures induces different macroscopic drainage behavior. Changing from one regime to another can be accomplished by changing the intrinsic rigidity of the surface layer at the foam bubble surface, but also by changing the bubble size [6–11]. The type of regime is determined by a "surface mobility" parameter M, which incorporate the different physical parameters that control foam drainage ($M = \frac{\mu r}{\mu_s}$, where μ is the bulk shear viscosity, μ_s the surface shear viscosity and r the radius of curvature of the PB); this parameter describes the coupling between the flow inside the PBs and at their surfaces [7, 9,11,12]. Measurements of the resistances to flow in the PBs and nodes, show that the resistance decreases with the surface mobility in the PBs, while the flow resistance in the nodes increases, and that both resistances are equal at the drainage regime transition [11].

The liquid bulk viscosity is included in the parameter M, and it should then also influence the foam drainage regime [12]. Up to now, there has been only a few experiments where the bulk viscosity was varied [13,14]. Recently, free-drainage experiments of viscous fluids, showed that a drainage transition can actually be induced by increasing the bulk viscosity, but no complete systematic studies were performed [8]. Investigating how foam drainage actually depends on viscosity, and the role that the bulk viscosity has in determining the foam drainage regime remain important issues.

Moreover, from the practical point-of-view, additives are often added to foaming solutions to eventually modify the foam properties, and to optimize the foam stability. These additives frequently change the solution viscosity,

[a] e-mail: saint-jalmes@lps.u-psud.fr

even providing solutions which are no longer Newtonian. In particular, it is usual to observe shear thinning behavior (decrease of the viscosity with the shear rate) with foaming fluids containing polymers [15]. Also, solutions containing specific long flexible polymers manifest nonlinear viscoelastic properties, such as large elongational viscosities and non-zero normal stress differences [15]. These specific rheological properties are responsible for many macroscopic effects, often already detected at low polymer concentrations, and which are not found for Newtonian fluids of similar shear viscosity [16]. Therefore, we have also investigated the role of theses polymers in foam drainage.

In this paper, we implement our previous preliminary work on the role of viscosity [14]. Together with a detailed analysis of how drainage depends on viscosity for Newtonian fluids, we add and compare new results on foams made with shear thinning fluids (adding polymers such as Carbopol and Xanthan), on foams made with elastic fluids (adding PolyEthylene Oxide) and on foams made with a set of Boger fluids (fluids having all the same shear viscosity, but different elongational ones).

2 Foam production and forced-drainage method

Foams are produced by bubbling nitrogen into the surfactant solution through porous glass cylinders. Different porosities are used in order to change the bubble diameters, D: four diameters have been studied, $D = 0.5$, 1, 2 and 4 mm. The nitrogen flow rate is adjusted to create homogeneous foams with small bubble size polydispersity, and traces of perfluorohexane (C_6F_{14}) are added to limit the bubble coarsening [17].

In this study, we have performed forced-drainage experiments [2]. First, a foam sample is allowed to dry under normal gravity conditions. Once the foam is dry, the same foaming solution is poured over the stationary foam at the top of the sample at controlled flow rates Q. We use the surface velocity $V_s = Q/S$, where S is the sample section to quantify our flow rates. In this configuration, a liquid front between a wet and a dry foam moves downward at a constant velocity V_f [2,3]. The motion of the front is monitored by electrical conductimetry [6,14], and multiple light scattering [8]. Typically, the front is followed over 30 cm, in the center of a foam column which is 70 cm height, to eliminate top and bottom boundary effects. The column cross section is 16 cm^2, so that there are always more than 10 bubbles in an horizontal section which ensure that wall effects are also negligible.

In forced-drainage models, the front velocity can be calculated considering that the liquid flows principally inside the interconnected network of PBs, linked together at the nodes. In a first limiting case, assuming immobile air-liquid interfaces, the flow in the PBs is then Poiseuille-like and the viscous dissipation essentially occurs in these PBs. The relation between V_f and V_s is given by [2,3]

$$V_f = \left(\frac{\rho g\, L^2}{\mu}\, K_{c0}\right)^{1/2} V_s^{1/2} \qquad (1)$$

where g is the acceleration of gravity, ρ the solution density, L the length of a PB, μ the bulk viscosity and K_{c0} is a dimensionless number describing the permeability of the rigid PB network. Regarding this permeability, first note that it is a useful quantity which directly describe the drainage velocity (for given bubble size and viscosity conditions), and secondly, it is also related to the hydrodynamic resistance of a PB, R_{c0}, as $R_{c0} \sim 1/K_{c0}$ [5,9,11]. K_{c0} has been theoretically estimated to be $K_{c0} = 1/150 \approx 6.6 \times 10^{-3}$ [3]. Assuming that the bubbles are monodisperse and are Kelvin tetrakaidecahedra, L can be related to the bubble diameter D *via* the relation: $D = c_1.L$, with $c_1 \approx 2.7$.

Oppositely, in a second limiting case, the bubble surfaces are mobile and the surface velocity is non-zero. Under such conditions, the flow in the PBs becomes more plug-like, and it has been proposed that the dissipation is then dominated by the one inside the nodes [4,5], leading to:

$$V_f = \left(\frac{\rho g\, L^2}{\mu}\, K_{n0}\right)^{2/3} V_s^{1/3} \qquad (2)$$

where K_{n0} is the permeability of the node network (the resistance R_{n0} of a node is here also proportional to the inverse of the permeability, $R_{n0} \sim 1/K_{n0}$ [5,11]). Preliminary numerical simulations [18] and experimental measurements [4,5,8,11] show that K_{n0} is of the same order of K_{c0}.

Experimentally, both limit regimes have been observed for different surface chemical compositions and different bubble sizes [3,4,6,7,11,19,20]. When the exponent α of the drainage curve ($V_f \sim V_s^{\alpha}$) is equal to 0.5 (within an error bar of ± 0.03) a permeability K_c can be calculated from the power law prefactor by using equation (1). In that limit, the nodes play no role, $K_n (\ll K_c)$ is not defined. When α is close to 1/3, a node permeability $K_n \gg K_c$ can be deduced from the power law prefactor. The conditions needed to obtain a given regime have recently been clarified: in a large range of experimental conditions, the surface mobility parameter $M = \frac{\mu r}{\mu_s}$ turns out to be the control parameter [7,11,20]. In the limit of dry foams, $r = c_2 D\sqrt{\varepsilon}$, ε being the liquid fraction, and $c_2 \approx 0.9$ [5]. M can then be written as: $M = c_2 \frac{\mu D\sqrt{\varepsilon}}{\mu_s}$; one can see here that it incorporates an interfacial parameter (emphasizing the role of 2D shear resistances), the bubble size, the bulk viscosity and the liquid fraction. The parameter M was first introduced by Leonard and Lemlich [12], and its role was discussed further recently by Desai and Kumar [21], Nguyen [22] and Koehler *et al.* [23]. For small M, the coupling between the surface and bulk flows is small, and the hydrodynamic resistance of the PBs dominates over the node resistance (in agreement with Eq. (1), $V_f \sim V_s^{1/2}$). Experiments and simulations show that increasing M decreases the resistance R_c of a PB, as a shear flow develops at the surface [7,11,22,23]. The effective permeability

K_c ($K_c \sim 1/R_c$) is thus not constant, and increases with M. This increase has been observed in experiments where M was changed by changing the bubble diameter, and a good agreement has been found between experiments and the predicted variations of K_{c0} [7,11,20,22,23]. At high enough M, the resistance of the PBs become smaller than the resistance of the nodes, and a drainage transition occurs. In the transition range, simple power law adjustments of forced drainage data (V_f *vs.* V_s) provide an exponent α between 1/3 and 1/2. In such cases, equations (1) and (2) cannot be used, but it is however possible to analyze the data by considering both contributions of PBs and nodes: the PBs and nodes hydrodynamics resistances are assumed to be in series [9], and this allows the separation of the two contributions (which consistently turn out to be of the same order) [9,11]. One can thus extract (not only in the limits where the exponent $\alpha = 1/2$ or 1/3), the values of the hydrodynamic resistances R_c, R_n (or permeabilities K_c, K_n) of both PBs and nodes. It is then possible to determine the contributions of flow across the different foam structural elements and get insights into the microscopic details of the liquid flow.

Another surface mobility parameter $N = \frac{\mu D_{\text{eff}}}{Er}$ where D_{eff} is an effective surfactant diffusion coefficient (including both interfacial and bulk contributions) and E the surface elasticity [24] has also been proposed, describing a different surface – bulk coupling (associated with surface tension gradients instead of surface shear in M), which may be important, for instance, when the bubbles are small.

As μ is included in both M and N, comparing experiments where μ is varied to previous results where the bubble size, or the surface viscoelasticity have been varied, could help in gaining a better understanding of drainage regimes transitions. Finally, let us stress that no specific drainage model or equations have been proposed yet for non-Newtonian fluids.

3 Materials and characterization

The chemicals were purchased from Aldrich, excepted when stated otherwise. Depending on the polymer added, we start either from a solution of an anionic surfactant, Sodium Dodecyl Sulfate (SDS) or from a solution of a cationic surfactant, tetradecyltrimethylammonium bromide (TTAB); the choice is made to prevent polymer-surfactant complexation at the surface and uncontrolled modification of the bulk and interfacial properties at the same time. We have added to all solutions a co-surfactant, dodecanol (DOH), to obtain high surface shear viscosities, and a well controlled and constant low interfacial mobility. For all solutions, the surfactant concentration is equal to 10 times the critical micellar concentration (cmc), and the surfactant/dodecanol weight ratio is fixed at 1000.

Glycerol-water volume percentages x were varied from 10 to 70%, and used with TTAB and DOH. Xanthan (from IDF) is a negatively charged natural polysaccharide, with a rigid backbone (molecular weight M_w is $\sim 10^5$ g/mol). Foams were made with mixed aqueous solutions of this polymer (concentrations between 0.15 and 0.3 g/L), of SDS (negatively charged surfactant, as the polymer) and of DOH. Another polymer, Carbopol (from BF Goodrich) was also used with SDS and DOH. Carbopol is a branched polyacrylic acid homopolymer, widely used as solution viscosifier (small amounts strongly increase the viscosity), and is known to form microgels in bulk. Carbopol concentration was varied between 0.2 g/L to 1 g/L. Polyethylene oxide (PEO) with different molecular weights ranging from 10^3 to 5×10^6 g/mol were used. The PEO concentration c was fixed to 3 g/L, excepted for the largest molecular weight where c was 0.75 g/L. PEO was used with TTAB and DOH, because it is known to form surface and bulk complexes with SDS. Finally, the composition of the so-called Boger fluids (PEO solutions in glycerol-water mixtures) is listed in Table 1.

Table 1. Composition and shear viscosity of the Boger fluids used in this study.

PEO molecular weight (g/L)	Composition PEO %(w/w)	Glycerol %(w/w)	Water %(w/w)	Viscosity (mPa.s)
6×10^5	0.270	20.00	79.730	4.99
1×10^6	0.150	5.00	74.850	4.56
5×10^6	0.080	15.00	84.920	4.70

The viscosity μ of the solutions is measured with a PAAR-Physica rheometer (MCR300), in a double gap Couette geometry, varying the shear rate between 1 to 200 s^{-1}. The viscosities of the glycerol-water solutions are all independent of the shear rate, as expected for a Newtonian fluid, and fall in the range 1 to 30 mPa.s. Figure 1 shows the flow curves (viscosity *vs.* shear rate) for the polymer solutions. For the solutions containing Carbopol (Fig. 1a), a moderate shear thinning behavior is observed at all concentrations. Pure Carbopol solutions have viscosities about 10 times higher than mixed Carbopol-SDS solutions, the surfactant inducing either a change in the bulk conformation of the polymer or a dispersion of the microgels. The shear thinning behavior is more marked with Xanthan than with Carbopol (Fig. 1b), as a result of the greater rigidity of the polymer backbone. Data for PEO solutions of different M_w are presented in Figure 1c. The shear viscosities are almost independent of shear rate, excepted for the two largest M_w polymers, where also a slight shear thinning effect is observed. The viscosities of the Boger fluids are almost independent of shear rate, even for the large PEO molecular weights and their values are reported in Table 1. Following these results, the Carbopol and Xanthan solutions can be considered as examples of shear thinning foaming fluids, whereas the PEO and Boger solutions represent the solutions having in addition some elastic properties and high elongational viscosities [15,16].

We have also measured the solution surface tensions, to check for eventual modifications of interfacial properties: a surfactant-polymer complexation at interfaces usually strongly decreases the surface tension, when compared to the pure surfactant system. The measurements are

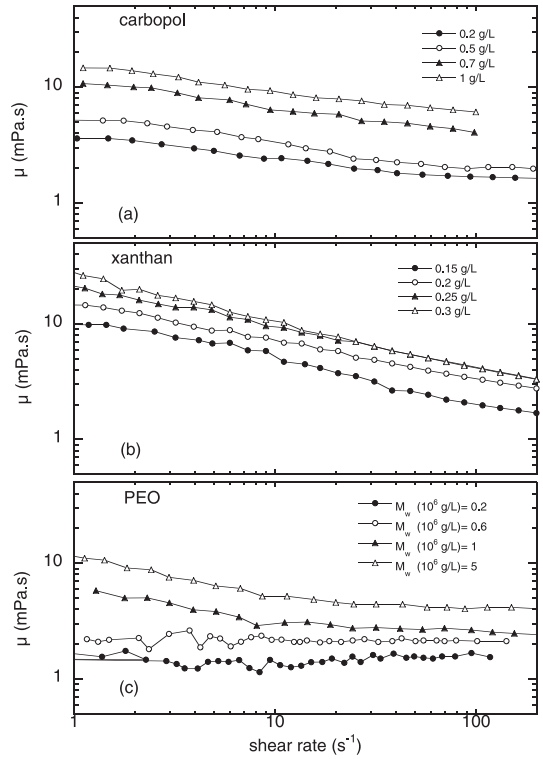

Fig. 1. Bulk shear viscosity μ as a function of the applied shear rate for (a) solutions containing SDS, DOH and Carbopol, (b) SDS, DOH and Xanthan, and (c) TTAB, DOH and PEO.

performed with a classical pendant drop tensiometer. For glycerol-TTAB solutions, no significant variations are detected up to 50% glycerol, and the surface tension γ remains close to 32 mN/m. Only for the percentage $x = 70\%$ is the surface tension slightly lower which is probably due to the amount of glycerol becoming dominant. For the solutions containing Carbopol, Xanthan and PEO, only slight decreases (up to 2 mN/m for the highest concentrations) have been observed. These data confirm that there are no, or only very little, surface complexation in our solutions, and no modification of the surface properties. Thus all the effects observed can only be due to modification of bulk properties, the interfaces being always in the low mobility limit.

4 Results

4.1 Newtonian foaming fluids: Glycerol-water mixtures

First, we recall that the solutions used here contained constant amounts of TTAB and DOH, chosen in order that the surfaces have large surface shear viscosities and large compression elasticities, hence intrinsically rigid surfaces. For a bubble diameter $D = 1 \pm 0.1$ mm, the forced-drainage curves for different glycerol percentages x have been modelled by power laws with exponents α. We have found that α remains close to 0.5 (0.5 ± 0.02) up to $x = 40\%$, then decreases: $\alpha = 0.43$ for $x = 50\%$ and $\alpha = 0.34$ for $x = 70\%$. For all the data up to $x = 50\%$,

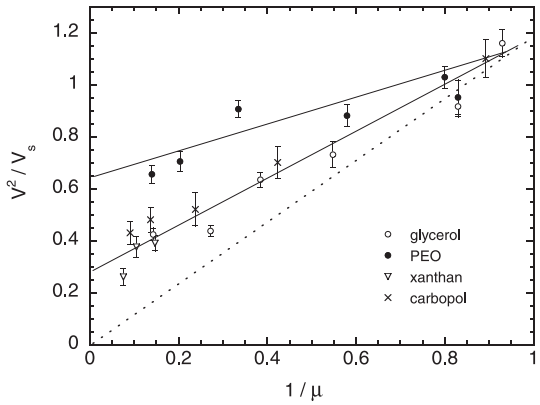

Fig. 2. Plot of V_f^2/V_s *vs.* $1/\mu$ for foams made of solutions containing glycerol, Carbopol, Xanthan or PEO. Bubble diameter D is 1 mm. For each system, the viscosity is varied either by changing the polymer concentration, or its molecular weight.

we have plotted V_f^2/V_s as a function of $1/\mu$ in Figure 2. The theoretical prediction (Eq. (1) with $K_c = 6.6 \times 10^{-3}$) is represented by the dashed line. Despite $\alpha \approx 0.5$ up to almost 50% of glycerol, it turns out that a significant deviation from the theory already appears at lower glycerol concentrations, and that the foams drain faster than expected. The same results can be presented in a different way, with the use of the permeabilities. The PB permeability K_c is plotted *vs.* μ in Figure 3 (normalized by the value found for the pure TTAB/DOH solution at $\mu = 1$ mPa.s, $K_c = 8 \times 10^{-3}$). For $\alpha \approx 0.5$, K_c is simply deduced via equation (1); while for $x = 50\%$, both a PB and a node contribution needs to be considered and the V_f *vs.* V_s needs to be fitted using a more complex equation form with two power law contributions [9,11] (then an associated node permeability $K_n = 7.8 \times 10^{-3}$ is found). One can then see that, in agreement with the curve of Figure 2, the PB permeability K_c is not constant and increases with μ, meaning that the resistance of the PBs decreases. It decreases finally so much with the viscosity that, for the 70% glycerol, only a node contribution is found: $\alpha = 0.34$, from which we get a single permeability $K_n = 12.0 \times 10^{-3}$.

We recall that, in these experiments, the bubble size ($D \approx 1$ mm) and the surface properties are kept constant, so that any change should be related to bulk properties. These data for Newtonian fluids will be used as a reference, to which the behavior of non-Newtonian fluids can be compared.

4.2 Solutions with Carbopol

For all the forced-drainage experiments with solutions made of SDS, DOH and Carbopol, and with a bubble size $D = 1 \pm 0.1$ mm, we have found that the drainage curves can be modelled with power laws with a exponent α from 0.45 to 0.5. In order to compare these results to those for Newtonian fluids, one first has to determine which single value of viscosity has to be ascribed to each Carbopol concentration. From the bubble size D, the measured average

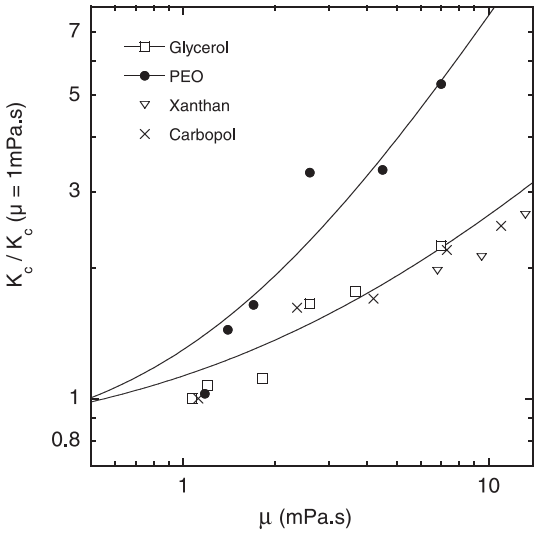

Fig. 3. Plateau border permeability K_c, normalized by the permeability of foams made with a TTAB/DOH solution of viscosity $\mu = 1$ mPa.s, as a function of bulk viscosity μ. The foams are made with solutions containing either glycerol, Carbopol, Xanthan and PEO.

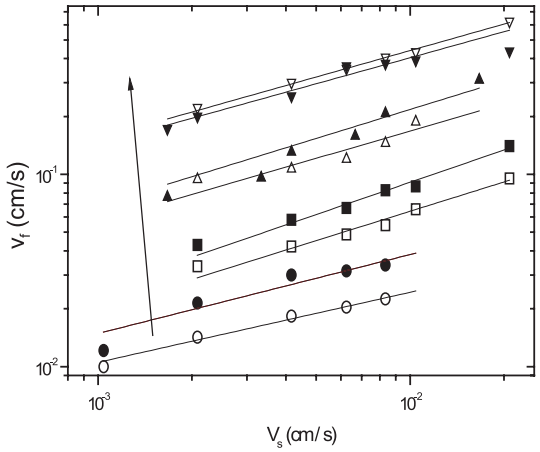

Fig. 4. Drainage front velocity as a function of the surface flowrate $V_s = Q/S$, for bubbles with different diameters (0.5, 1, 2 and 4 mm) with glycerol (open symbols) and PEO solutions (full symbols). In the first case the percentage of glycerol is $x = 45\%$; in the second, the concentration of PEO is $c = 3$ g/L ($M_w = 10^6$ g/mol). Both solutions have the same shear viscosity, $\mu \approx 4.6$ mPa.s. The arrow indicates the increase of the bubble size.

liquid fractions and liquid velocities v at each concentration, it is possible to determine the PB section r (using $r = c_2 D\sqrt{\varepsilon}$), the shear rate $\dot{\gamma}$ within these PBs ($\dot{\gamma} \sim v/r$), and thus finally the effective viscosity from the curves of Figure 1. We find that the local shear rates $\dot{\gamma}$ in the foam are in the range 3 to 8 s^{-1}. Once plotted as a function of these effective viscosities (Fig. 2), we find that the results for the Carbopol coincide well with the data for the glycerol solutions. Consequently, the Carbopol permeability data fall on the same curve than the glycerol data (Fig. 3). This shows that our estimation of the effective shear rates (and thus viscosity) inside the foam are correct, and that the shear-thinning behaviour of Carbopol solutions does not change the physical mechanisms of drainage.

4.3 Solutions with Xanthan

Xanthan solutions have a more pronounced shear-thinning behaviour than Carbopol solutions. For the three lowest concentrations of Xanthan, the forced drainage curve exponent is close to 0.5: $\alpha = 0.48 \pm 0.02$. We calculated and reported in Figures 2 and 3 the quantities V_f^2/V_s and K_c, using effective viscosities deduced from the local shear rates (as for the Carbopol solutions). Here again, the Xanthan results are close to those for glycerol and Carbopol. For the highest concentration of Xanthan, $c = 0.3$ g/L, we have found an exponent $\alpha = 0.35$, as for glycerol with $x = 70\%$. Here the local viscosity is $\mu = 15$ mPa.s. Using equation (2), we have calculated a node permeability $K_n = 10.5 \times 10^{-3}$, close to that measured for glycerol. Again therefore, the shear-thinning behaviour of the foaming solution does not change the drainage mechanisms.

4.4 Solutions with PEO

For all the solutions containing TTAB, DOH and PEO, the exponents from the drainage curves are close to 0.5. So, it is here also relevant to look at the variation of V_f^2/V_s with of $1/\mu$. As for the other solutions, we take an average value over typical local shear rates found in the foam. For the smallest PEO molecular weights, drainage velocities are close to those for glycerol-water mixtures with the same μ. However, for larger molecular weights (thus higher viscosities), the behavior of the PEO solutions is significantly different, and the drainage is faster than for all the other solutions having the same bulk viscosity (Fig. 2). This translates into differences in permeability K_c (Fig. 3): for PEO, K_c can be twice as large as that for Newtonian or shear-thinning fluids.

In order to find the origin of these differences, we have varied the bubble diameter. Changing the bubble size is a way to change the average flow velocity, and therefore to change local hydrodynamic stresses (both shear and elongational) in foams. Note that the foam liquid fraction above the front also changes, from 0.7% (for the largest bubbles and the smallest flow rates) to around 20% (for the smallest bubbles, and largest flow rates, just before the occurrence of convective instabilities). We have selected 2 solutions having the same bulk viscosity ($\mu = 4.6$ mPa.s): a 45% glycerol solution and a 3 g/L PEO solution with $M_w = 10^6$ g/mol. The bubble diameter is then varied from 0.5 to 4mm (Fig. 4). For the smallest bubbles, the PEO-based foams always drain faster than the glycerol based ones. However, the difference between drainage velocities continuously decreases as the bubble diameter is increased, and finally vanishes for the largest bubbles, $D = 4$ mm.

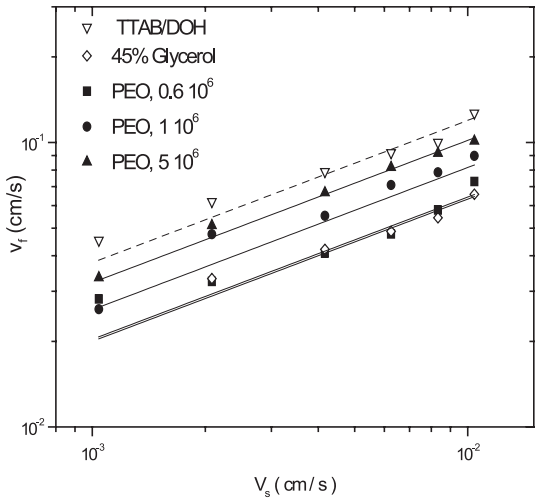

Fig. 5. Drainage curves for the foams made with Boger solutions. The results for the pure surfactant solution and for a Newtonian solution with glycerol ($x = 45\%$) are also plotted for comparison. Bubble diameter is 1 mm.

Note that we see here an effect of bubble size, already found in previous studies: the exponent of the drainage curves, close to 0.5 for intermediate bubble size (1 mm diameter), decreases towards 0.35 for smaller and larger bubbles, confirming that drainage regime transitions can be induced by bubble size changes [8,11].

4.5 Boger fluids: PEO/glycerol/water mixtures

When changing the PEO molecular weight, one changes both shear and elongational properties of the solutions. In order to disentangle these contributions, we have studied a series of foams made with Boger fluids. These fluids are dilute PEO solutions in glycerol-water mixtures of variable composition (see Tab. 1). The interest here is that their shear viscosities are identical, whereas the elongational ones are changed.

The drainage curves for the three Boger fluids are reported in Figure 5, together with the result for the Newtonian solution with the same shear viscosity (TTAB/DOH with 45% glycerol). Here again, the exponent α is close to 0.5 (main resistance always within the PBs). The foams with PEO of small M_w (0.6×10^6 g/mol) drain with the same velocity than with the equivalent Newtonian fluid (45% glycerol). But when the PEO molecular weight is increased, the drainage is significantly faster. One can also see that the increase in drainage velocity is larger when the PEO molecular weight increases from 0.6×10^6 to 10^6, than when it increases from 10^6 to 5×10^6: the velocity does not increase linearly with M_w, and tends to saturate as M_w increases. In relation to this saturation, it is striking to note that for the highest M_w investigated here, it is almost possible to increase the velocities up to the ones obtained with a glycerol-free surfactant solution having a bulk viscosity of 1 mPa.s (thus about 5 times smaller than that of the Boger fluid, dashed line in Fig. 5).

We finally point out that, for a fixed bulk viscosity, the maximum increase of the PB permeability K_c with Boger fluids is close to the one found with the PEO solutions: K_c is multiplied by a factor close to 2, when compared to the results for Newtonian fluids.

5 Discussion

5.1 Surfactant solutions with glycerol, Xanthan and Carbopol

Regarding their effects on drainage, foaming solutions containing glycerol, Carbopol or Xanthan share the same properties, whether these fluids are Newtonian or not. The surface viscoelasticity being kept high and constant, the drainage velocity varies with μ but does not follow equation (1). As μ is increased, α decreases down to 0.34, and the PB permeability K_c increases (meaning a continuous decrease of the hydrodynamic resistance of the PBs). These features are similar to the drainage regime transition seen when surface viscoelasticity or bubble size are varied [6,8,11]. So the coupling between surface flow and bulk flow in the PBs can also be tuned by the bulk viscosity, as expected since the control parameters M and N depend on μ, and a transition in drainage regime is clearly found as μ is increased. For the bubble size tested here, the critical viscosity range, corresponding to the crossover from one regime to the other, appears to be between 12 and 20 mPa.s.

At this stage, a first analysis consists to compare the observed variations of K_c with μ, to the available models [21,23]: models predict the dependence of K_c with M, $Kc(M) \approx K_{c0}\ (1 + sM)$ with $s = 2.4$, from which we also get $Kc(\mu)$ (note that as there are no predictions for $Kc(N)$, similar comparisons cannot be done). From the value of K_c for $\mu = 1$ mPa.s ($K_c \approx 8\times10^{-3}$), we extract a value of $M \approx 0.2$, corresponding to a surface viscosity $\mu_s = 6\times10^{-4}$ g s^{-1}. This value of μ_s is in agreement with previous determinations from other forced-drainage experiments [7,11,19]. As μ is varied within a decade (adding either glycerol, Carbopol or Xanthan), M spans a range from 0.2 to 2. The measured variation of K_c is significantly smaller than predicted by the models when M varies in that range: it is still possible to fit the permeability data by a functional form $K_{c0}(1+s\mu)$ (solid line in Fig. 3), but s is finally a factor 1.75 smaller than the prediction. One can also note that according to the model, the transition to the regime $\alpha = 1/3$ should have taken place with viscosities $\mu \approx 10$ mPa.s, for which $M > 1$. Finally, beyond the transition, once $\alpha \approx 1/3$ for large μ, the measured permeabilities K_n are 4 times larger than those reported before ($K_n \approx 3\times10^{-3}$) [4,5,11]. This suggests that the viscosity-induced transition does not fit well with this model, and thus with the underlying microscopic mechanism linked to the parameter M.

It is interesting to note that there are similarities between the drainage transitions observed when μ is increased and when the bubble size is decreased (for instance, the same $K_n = 10\times10^{-3}$ is found in both cases

above the transition) [11]. High viscosities or small bubble sizes correspond to high values of N, and one can thus wonder if these transitions could be controlled by this parameter. Quantitatively, N remains quite small under these experimental conditions (on the order of 10^{-3}–10^{-4}), so the corresponding surface tension gradients should have negligible effects. Nevertheless, as discussed in [25], some effects apparently controlled by N seem indeed to occur while N is as small as here. Of course, this discussion cannot lead to the conclusion that N controls the high viscosity or the small bubble drainage regimes. The microscopic mechanisms involved in this viscosity-induced drainage transition, and the drainage features for high bulk viscosities, still require an explanation. Data reported here, as well as those on single PB [19] where the effect of Newtonian bulk viscosity has also been studied, will now be useful for comparisons to future models.

5.2 Surfactant solutions containing PEO

The foams made with PEO solutions of large enough molecular weight drain faster than foams made with Newtonian liquids of the same shear viscosity. This is a rather counter-intuitive result, since PEO solutions resist both shear and elongational deformations, and one might expect slower drainage due to cumulative shear and elongational dissipation. Indeed, in solid porous media, long flexible polymers such as PEO increase pressure drops whatever the flow rate imposed [26]. The effect seen here appears to be specific to foams: the main difference between a foam and a solid porous media is that the foam pore sizes (PBs sections) are not constant. The PB sections, their geometry (as well as those of the nodes) depend on the liquid fraction, and are dynamically adjusted to the flow properties. This adaptability of the liquid network is certainly a first important ingredient for explaining our observations. It is interesting to note that isolated foam films drain faster when made with PEO solutions than with Newtonian fluids of similar viscosity [27]. Here also, the shape of the thin film and of its meniscus changes during liquid flow.

PEO solutions and Boger fluids have non-linear responses to elongational strains. Their high elongational viscosities originate from the viscous resistance occurring when the polymer chains are stretched. The fact that for the elastic fluids, drainage is faster than with Newtonian fluids suggests that elongational properties play a role. This is even more clear with the Boger fluids results: when we have increased only the elongational fluid properties (all the rest being constant), the drainage speed increases.

There are usually no elastic effects at low elongational deformation rates. Let us consider the simple case of sink flow through a contraction in a cylindrical pipe: the elongational rate depends on the liquid velocity, on the pipe section radius and on the contraction angle [28]. By applying this picture to foams, one can crudely estimate elongational rates between 1 and 10 s^{-1}. Note also that the elongation might be only located in a thin fluid layer near the PB surfaces (as often found in such contraction problems); then the correct length scale associated to the elongation could be much smaller than the PB radius, implying even higher elongational rates in the foam. Recent results by Pelletier *et al.*, with the opposing jets method, show that non-Newtonian effects occur much sooner than previously expected, and that deformation of the coil can occur at very low strain rates, typically a decade lower than the strain rate predicted for the coil-stretch transition [29]. Pelletier *et al.* found that for polyacrylamide solutions of $M_w = 10^6$g/mol, the critical strain is typically around 5 s^{-1} [29]. This suggests that elongational strains could be just high enough in PBs during forced-drainage to change flow mechanisms.

We can then only speculate on how the elastic properties of the fluid can modify the microscopic flow, and thus the macroscopic drainage velocities. It is possible that another ingredient to add is that the elongational viscosity increases with the elongational strain rates [15,28]. This property, known as "tension-thickening", stabilizes liquid filaments against abrupt changes in diameter [15]. Such diameter changes imply locally a maximum of elongational rate, and thus local higher stresses due to this tension thickening effect: the flow then react by smoothing out the section change to reduce the stresses [15]. This tension-thickening effect provides a link between the adjustable PB geometry and the elastic properties of the fluid. In a foam made with an elastic fluid, the PB shape and cross section, as the liquid filament ones, could adapt to reduce local elongational stresses, occurring as soon as there are wide section changes (especially within the drainage front), by smoothing these sections changes. Such modifications of the geometry must then have an impact on the liquid velocity (for a given injected flowrate and due to mass conservation, the liquid velocity is higher if the channel section is smaller). Note that as the node shape is also adjustable, geometrical changes balancing elongational stresses probably also occur in the nodes, and this may also affect the final velocity. These effects obviously do not exist in solid porous media. This adaptation is also not needed for a Newtonian fluid, for which there are no elongational stresses.

Preliminary experiments on a single PB held on a solid frame, and with a high speed camera, actually show that the PB shape is modified in the presence of PEO: in agreement with these ideas, the change of cross section is smoother with PEO, the contraction is smaller and the length over which the section changes is larger.

The effect of bubble size shown in Figure 4 remains difficult to explain and more work is needed to clarify this issue.

6 Conclusions

We have studied the role of the bulk viscosity on foam drainage. It is first found that a drainage regime transition can be induced by increasing the bulk viscosity. The way the transition is approached and crossed is well identified, and turn out to be different from what is found

when surface properties are varied. The viscosity-induced transition in fact appears more similar to the transition seen when the bubble size is decreased.

If non-Newtonian foaming solutions are used, the properties of drainage are not affected by the shear-thinning behavior of these solutions. If one ascribes an effective viscosity, corresponding to the estimated local shear rate inside the foam, the velocity of drainage is the same than for Newtonian fluids at the same viscosity.

Experiments with solutions containing PEO and PEO-based Boger fluids led to unexpectedly high foam drainage velocities, the elastic properties of these fluids having a counter-intuitive impact on drainage. We have proposed here some elements of understanding, identifying which properties of the foam itself and of the solutions may have to be taken into account. Nevertheless, this effect remains to be explained in details, and further works are in progress.

This work has been supported in part by the Centre National d'Études Spatiales (CNES) and the European Space Agency (ESA); we also thank O. Pitois and V. Bertola for useful discussions.

References

1. D. Weaire, S. Hutzler, *The Physics of Foams* (Oxford University Press, Oxford, 1999)
2. N. Pittet, S. Hutzler, D. Pardal, D. Weaire, Phys. Rev. Lett. **71**, 2670 (1993)
3. D. Weaire, S. Hutzler, G. Verbist, E. Peters, Adv. Chem. Phys. **102**, 315 (1997)
4. S.A. Koehler, S. Hilgenfeldt, H.A. Stone, Phys. Rev. Lett. **82**, 4232 (1999)
5. S.A. Koehler, S. Hilgenfeldt, H.A. Stone, Langmuir **16**, 6327 (2000)
6. M. Durand, G. Martinoty, D. Langevin, Phys. Rev. E **60**, R6037 (1999)
7. S.A. Koehler, S. Hilgenfeldt, E.R. Weeks, H.A. Stone, Phys. Rev. E **66** (2002) 040601(R)
8. A. Saint-Jalmes, D. Langevin, J. Phys. Condens. Mat. **14**, 9397 (2002)
9. H.A. Stone, S.A. Koehler, S. Hilgenfeldt, M. Durand, J. Phys. Condens. Mat. **15**, S283 (2003)
10. D. Weaire, S. Hutzler, S. Cox, N. Kern, M.A. Alonso, W. Drenckhan, J. Phys. Condens. Mat. **15**, S65 (2003)
11. A. Saint-Jalmes, Y. Zhang, D. Langevin, Eur. Phys. J. E **15**, 53 (2004)
12. R.A. Leonard, R. Lemlich, AICh.E. Journal **11**, 18 (1965)
13. S. Stoyanov, C. Dushkin, D. Langevin, D. Weaire, G. Verbist, Langmuir **14**, 4663 (1998)
14. M. Safouane, M. Durand, A. Saint-Jalmes, D. Langevin, V. Bergeron, J. Phys. IV (France) **11**, Pr6 –275 (2001)
15. H.A. Barnes, J.F. Hutton, K. Walters. *An Introduction to Rheology* (Amsterdam, Elsevier, 1989)
16. R.B. D Bird, R.C. Armstrong, O. Hassager, *Fluid Mechanics*, Dynamics of Polymeric Liquids, Vol. 1 (Wiley, New York, 1987); W.D. MacComb, *The physics of Fluid turbulence* (Clarendon, Oxford, 1990); A. Gyr, H.-W. Bewersdorf, *Drag reduction of Turbulent Flows and Additives* (Kluwer, Dordrecht, 1995); A. Groisman, V. Steinberg, Phys. Rev. Lett. **77**, 1480 (1996); D. Bonn, J. Meunier, Phys. Rev. Lett. **79**, 2662 (1997); V. Bergeron, D. Bonn, J.Y. Martin, L. Vovelle, Nature **405**, 772 (2000)
17. F.G. Gandolfo, H.L. Rosano, J. Colloid Interface Sci. **194**, 31 (1997)
18. S.J. Cox, G. Bradley, S. Hutzler, D. Weaire, J. Phys. Condens. Mat. **13**, 4863 (2001)
19. O. Pitois, C. Fritz, M. Vignes-Adler, Coll. Surf. A **261**, 109 (2005)
20. S.A. Koehler, S. Hilgenfeldt, E.R. Weeks, H.A. Stone, J. Colloid Interface Sci. **276**, 439 (2004)
21. D. Desai, R. Kumar, Chem. Eng. Sci. **37**, 1361 (1982)
22. A.V. Nguyen, J. Colloid Interface Sci. **249**, 194 (2001)
23. S.A. Koehler, S. Hilgenfeldt, H.A. Stone, J. Colloid Interface Sci. **276**, 420 (2004)
24. M. Durand, D. Langevin, Eur. Phys. J. E **7**, 35 (2002)
25. G. Singh, G.J. Hirasaki, C.A. Miller, J. Colloid Interface Sci. **184**, 92 (1996)
26. R.W. Dexter, Atomization Sprays **6**, 167 (1996); F. Durst, R. Haas, B.U. Kaczmar, J. App. Pol. Sci. **26**, 3125 (1981); W.M. Kulicke, Ind. Eng. Fundam. **23**, 308 (1984)
27. S. Cohen-Addad, J.M. DiMeglio, Langmuir **10**, 773 (1994)
28. C.W. Macosko, Extensional Rheometry, in *Rheology, Principles, Measurements and Applications* (VCH Publishers, New York, 1994)
29. E. Pelletier, C. Viebke, J. Meadows, P. Williams, Langmuir **19**, 559 (2003)